DOI:10.1093/jnci/dju050
First published online April 28, 2014

ARTICLE

Amplification of TRIM44: Pairing a Prognostic Target With Potential Therapeutic Strategy

Chin-Ann Johnny Ong, Nicholas B. Shannon, Caryn S. Ross-Innes, Maria O'Donovan, Oscar M. Rueda, De-en Hu, Mikko I. Kettunen, Christina Elaine Walker, Ayesha Noorani, Richard H. Hardwick, Carlos Caldas, Kevin Brindle, Rebecca C. Fitzgerald

Manuscript received July 9, 2013; revised January 24, 2014; accepted February 3, 2014.

Correspondence to: Rebecca Fitzgerald, MD, FRCP, FMedSci, MRC Cancer Unit, Hutchison/MRC Research Centre, Hills Rd, Cambridge, CB2 0XZ, UK (e-mail: rcf29@hutchison-mrc.ac.uk).

Background Many prognostic biomarkers have been proposed recently. However, there is a lack of therapeutic strategies exploiting novel prognostic biomarkers. We aimed to propose therapeutic options in patients with overexpression of TRIM44, a recently identified prognostic gene.

Methods Genomic and transcriptomic data of epithelial cancers (n = 1932), breast cancers (BCs; n = 1980) and esophagogastric cancers (EGCs; n = 163) were used to identify genomic aberrations driving TRIM44 overexpression. The driver gene status of TRIM44 was determined using a small interfering RNA (siRNA) screen of the 11p13 amplicon. Integrative analysis was applied across multiple datasets to identify pathway activation and potential therapeutic strategies. Validation of the in silico findings were performed using in vitro assays, xenografts, and patient samples (n = 160).

Results TRIM44 overexpression results from genomic amplification in 16.1% of epithelial cancers, including 8.1% of EGCs and 6.1% of BCs. This was confirmed using fluorescent in situ hybridization. The siRNA screen confirmed *TRIM44* to be a driver of the amplicon. In silico analysis revealed an association between TRIM44 and mTOR signalling, supported by a decrease in mTOR signalling after siRNA knockdown of TRIM44 in cell lines and colocalization of TRIM44 and p-mTOR in patient samples. In vitro inhibition studies using an mTOR inhibitor (everolimus) decreased cell viability in two *TRIM44*-amplified cells lines by 88% and 70% compared with 35% in the control cell line. These findings were recapitulated in xenograft models.

Conclusions Genomic amplification drives TRIM44 overexpression in EGCs and BCs. Targeting the mTOR pathway provides a potential therapeutic option for *TRIM44*-amplified tumors.

JNCI J Natl Cancer Inst (2014) 106(5): dju050 doi:10.1093/jnci/dju050

During the past few decades, advances in microarray and sequencing technology have provided a detailed map for understanding the cancer genome. Many studies have attempted to correlate this enhanced knowledge with clinical parameters, including survival. It is hoped that patients who have been molecularly stratified into prognostic subgroups can be selected for specific therapy in clinical practice (1–5). Examples of successful targeted agents include imatinib and inhibitors targeting Her2, EGFR, and B-raf. These drugs provide clinical benefit in patients with specific genomic alterations, such as activating mutations, fusion genes, or copy number aberrations (6–11). However, prognostic signatures often identify genes with no known function. Therefore more work is needed to identify therapeutic strategies relevant to these poorly understood molecular aberrations.

We have previously identified and validated that the gene tripartite motif containing 44 (*TRIM44*) is a prognostic target in three esophago-gastric cancer (EGC) cohorts comprised of 1040 patients (12). This is supported by a recent publication suggesting that gastric cancers with TRIM44 overexpression are more aggressive (13). TRIM44 belongs to a family of 70 proteins involved in diverse pathological conditions, including developmental disorders, neurodegenerative diseases, and viral infections (14). Increasingly, members of the TRIM family have been found to be involved in oncogenic processes through transcriptional regulation, cellular proliferation, and apoptosis (15). However, the functional role and therapeutic potential of TRIM44 in cancer has not been elucidated.

The aims of this study were as follows: 1) determine the timing and prevalence of TRIM44 overexpression to allow focusing on the appropriate genomic resource; 2) understand the genetic basis driving TRIM44 overexpression; 3) determine the consequence of dysregulation of TRIM44 on signalling pathways; and 4) formulate a therapeutic strategy targeting TRIM44-overexpressing tumors.

Methods

Human Tissue Samples

All human samples were collected after institutional ethics board approval and individual informed consent (01/149, 07/H0305/52, LREC01/149). Cancer samples used were described in a previous study (tissue microarray: n = 349; gene expression: n = 75) (16). Paraffin slides of tumor-positive lymph nodes were available in 99 of 349 patients. Samples consisting of Barrett's esophagus with no dysplasia (n = 117), low-grade dysplasia (n = 30), and high-grade dysplasia (n = 62) were from an independent cohort. Genomic and transcriptional data analysis was performed on epithelial cancers (n = 1932), breast cancers (BCs; n = 1980) and EGCs (n = 163). We have included a summary of the number of patients, genomic platforms used, and analysis done for each cohort in the Supplementary Table 1 (available online).

Immunohistochemistry and Immunofluorescence

Immunohistochemistry was performed on a Bond System (Leica Microsystems, Milton Keynes, UK). Antibody sources and conditions used for immunohistochemistry and scoring criteria are detailed in the Supplementary Methods and supplementary table 3 (available online). The detailed immunofluorescence protocol is described in the Supplementary Methods (available online).

Western Blot

Protein from whole cells was extracted using lysis buffer containing 0.3 M sodium chloride, 1% (v/v) Triton X-100, and 50 mM Tris pH 8.0 supplemented with ProteaseComplete (Roche) protease and PhosphoSTOP (Roche) phosphatase inhibitors. Western blotting was performed as described in the Supplementary Methods and supplementary table 4 (available online).

Generation of Metaphase Spreads and Fluorescent In Situ Hybridization

Preparation of metaphase spreads and the detailed fluorescent in situ hybridization (FISH) protocol are described in the Supplementary Methods (available online).

FISH on Tissue Microarrays

Labelling of BAC probes (detailed in Supplementary Methods, available online) was performed using the Nick translation kit (Abbott Molecular, Des Plaines, IL, USA). FISH on paraffin samples was performed using the citric acid buffer method. The detailed protocol is described in the Supplementary Methods (available online).

Small Interfering RNA Screen and Cell Inhibition Studies With Inhibitors

Cells were transfected with four independent small interfering RNAs (siRNAs) targeting all genes in the 11p13 amplicon using Hiperfect (Qiagen, Crawley, UK). The sequences of the siRNA are detailed in the Supplementary Methods (available online). Cellular proliferation after siRNA treatment was assessed after 72 hours using the CellTitreGlo assay (Promega, Madison, WI, USA) and a plate luminescence reader (Tecan; Perkin-Elmer, Waltham, UK). Cell inhibition studies were performed as previously described (17) using everolimus (Sigma-Aldrich, Poole, UK), PP242 (Stratech Scientific Limited, Suffolk, UK), and wortmannin (Calbiochem, Nottingham, UK).

Gene Expression Profiling

Gene expression profiling after siRNA knockdown of TRIM44 was performed in the Genomics CoreLab in Addenbrooke's Hospital using GeneChip Gene ST 1.0 arrays (Affymetrix, Wycombe, UK). Normalized expression estimates were obtained from raw intensity values using a probe level linear model preprocessing algorithm available in the Bioconductor library AffyPLM (fitPLM) using default settings.

Gene Set Enrichment Analysis

Gene sets were chosen from version 3.0 of the molecular signatures database (MSigDB) (18), selecting single gene sets representing upregulated genes after direct pathway activation (n = 20). The analysis was performed on EGC (Kim (25): n = 64, Greenawalt (26): n = 37) and breast cancer (METABRIC (21): n = 1980), supplementary table 2. Because the false discovery rate adjustment was too conservative in the esophageal datasets, and because we wished to be inclusive in the discovery phase, statistically significant enrichment was taken as a nominal P value less than .05. Gene set enrichment analysis (GSEA) was also performed to validate signature changes with TRIM44 siRNA. The mTOR signature referred to in the article is the "PARENT MTOR SIGNALLING UP" signature (19).

Connectivity Map Analysis

Expression data from HSC39 treated with TRIM44 siRNA was used to rank genes for association with TRIM44 using a signal-to-noise metric (difference of means scaled by the standard deviation). The top and bottom 1% of differentially expressed genes were used to query the connectivity map (20) and identify any bioactive molecules showing changes antagonistic to a TRIM44 transcriptional signature (positive enrichment in connectivity map analysis).

METABRIC Data Analysis

The details of the METABRIC dataset could be obtained from the original manuscript (21). The effect of copy number alterations on expression and breast cancer–specific survival was evaluated using one-sided Jonckheere–Terpstra test and Kaplan–Meier estimates with log-rank testing, respectively. Statistical significance was defined as P less than .05.

Xenografts

Tumors were implanted into BALB/c male nude mice (aged 6–8 weeks; Charles River, Margate, UK) by subcutaneous injection in the lower flank using 5×10^6 cells. Tumors were allowed to grow for 14 days before treatment. Two hundred microliters of vehicle or everolimus (10 mg/kg; Seqoia, Pangbourne, UK) was administrated through oral gavage daily. Tumor volume was measured with callipers until day 24. Magnetic resonance imaging was performed on day 23 before animals were killed. For MRI imaging, animals were anesthetized with intraperitoneal Hypnorm (VetaPharma)/Hypnovel (Roche)/dextrose-saline (4%:0.18%, wt/vol) in a 5:4:31 ratio (10 mL/kg of body weight) and kept warm by blowing warm air through the magnet bore during the experiment. All experiments were conducted in compliance with project and personal licenses issued under the Animals (Scientific Procedures) Act of 1986 and were designed with reference to the UK Co-ordinating Committee on Cancer Research guidelines for the welfare of

animals in experimental neoplasia. The work was approved by a local ethical review committee.

Magnetic Resonance Imaging

Transverse T_2- (repetition time = 1.5 s; echo time = 40 ms) and T_1-weighted (repetition time = 0.4 s; echo time = 10 ms) ^1H images were acquired at 9.4 T using a spin-echo pulse sequence ($40 \times 40\ mm^2$ field of view; data matrix 256×128; 21 slices with slice thickness of 1.5 mm and no gaps between slices). The tumor volume was estimated from magnetic resonance images by manually selecting a region of interest covering tumor in each slice and multiplying the total tumor area with the slice thickness.

Statistical Analysis

The χ^2 test and Fisher exact tests were used to compare TRIM44-overexpressing samples in EGC pathogenesis and p-mTOR staining in amplified vs nonamplified samples. The strength of the effect of the copy number alterations on the expression profiles was evaluated using the Jonckheere–Terpstra test. Survival analysis was performed using the log-rank test. Statistical analysis on functional assays was performed using the unpaired *t* test. The *P* values for the enrichment analysis were generated using GSEA software, which is based on an ad hoc modification of the Kolmogorov-Smirnov test (KS) test. The *P* values used for the connective map analysis are generated using cmap, which is based on an ad hoc modification of the KS test All statistical tests were two-sided unless stated. Differences were considered statistically significant at a *P* value less than .05.

Results

TRIM44 Overexpression in EGC Pathogenesis

Events occurring just before invasion are likely to be important steps in malignant transformation (22,23). Therefore, we first sought to establish the timing of overexpression by exploiting the fact that EGC develops through a metaplasia–dysplasia–carcinoma sequence (22). TRIM44 overexpression was present in 27.3% of Barrett's esophagus (n = 117), 33.3% of low-grade dysplasia (n = 30), and 51.6% of high-grade dysplasia (n = 62). The frequency of TRIM44 overexpression in high-grade dysplasia was similar to that of EGC (56%; n = 349; (12)) and was statistically significantly higher than in patients with Barrett's esophagus (Figure 1A). In an exemplar case where EGC had demonstrably arisen from Barrett's esophagus, TRIM44 expression was increased in the stages between Barrett's esophagus and high-grade dysplasia and to EGC, further supporting our findings (Figure 1B). High expression of TRIM44 in metastatic cells in lymph nodes also conferred a poorer prognosis to patients (Figure 1C).

Prevalence of TRIM44

Analysis of our gene expression data of 75 EGCs (16) demonstrated a "stepladder" increase in TRIM44 expression in a small subset of tumors, hinting at an underlying genomic aberration (Figure 2A). Interrogation of publicly available genomic data revealed that the *TRIM44* locus was amplified in 16.1% of all epithelial cancers (n = 1932) in Tumorscape (24) (Table 1). Furthermore, 4.0% of all epithelial cancers harbored focal amplifications of *TRIM44*, making it a candidate driver gene (Figure 2B). Eighteen of 88 of the EGC samples on Tumorscape had *TRIM44* amplifications and gains. FISH performed on tissue microarray of EGCs validated that 8.1% of EGCs (n = 13 of 160) had *TRIM44* gains and amplifications (Figure 2C). Immunohistochemistry performed on these samples revealed that increase in copy number was enriched for

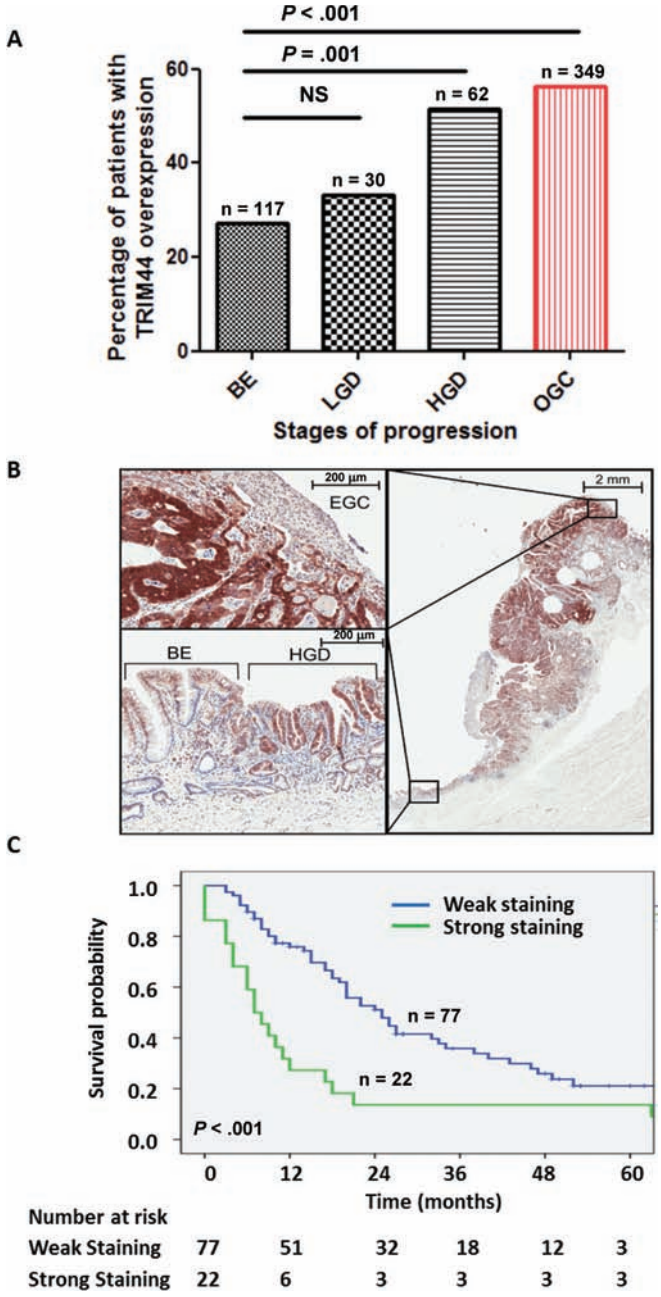

Figure 1. TRIM44 expression in esophago-gastric cancers (EGCs). **A**) Percentage of patients with TRIM44 overexpression in different stages of the pathogenesis of EGC. *P* value computed by two-sided χ^2 test. Percentage of TRIM44 overexpression in EGC samples was extracted from our previous publication (12) (n = 349). BE = Barret's esophagus; LGD = low-grade dysplasia; HGD = high-grade dysplasia; NS = not statistically significant. **B**) Representative immunohistochemistry pictures of one case with adjacent Barrett's esophagus (BE) with no dysplasia, HGD, and EGC. **C**) Kaplan–Meier curve comparing survival of patients with TRIM44-positive cancer cells in metastatic lymph nodes with patients with TRIM44-negative cancer cells in the metastatic lymph nodes (*P* value computed by two-sided log-rank test).

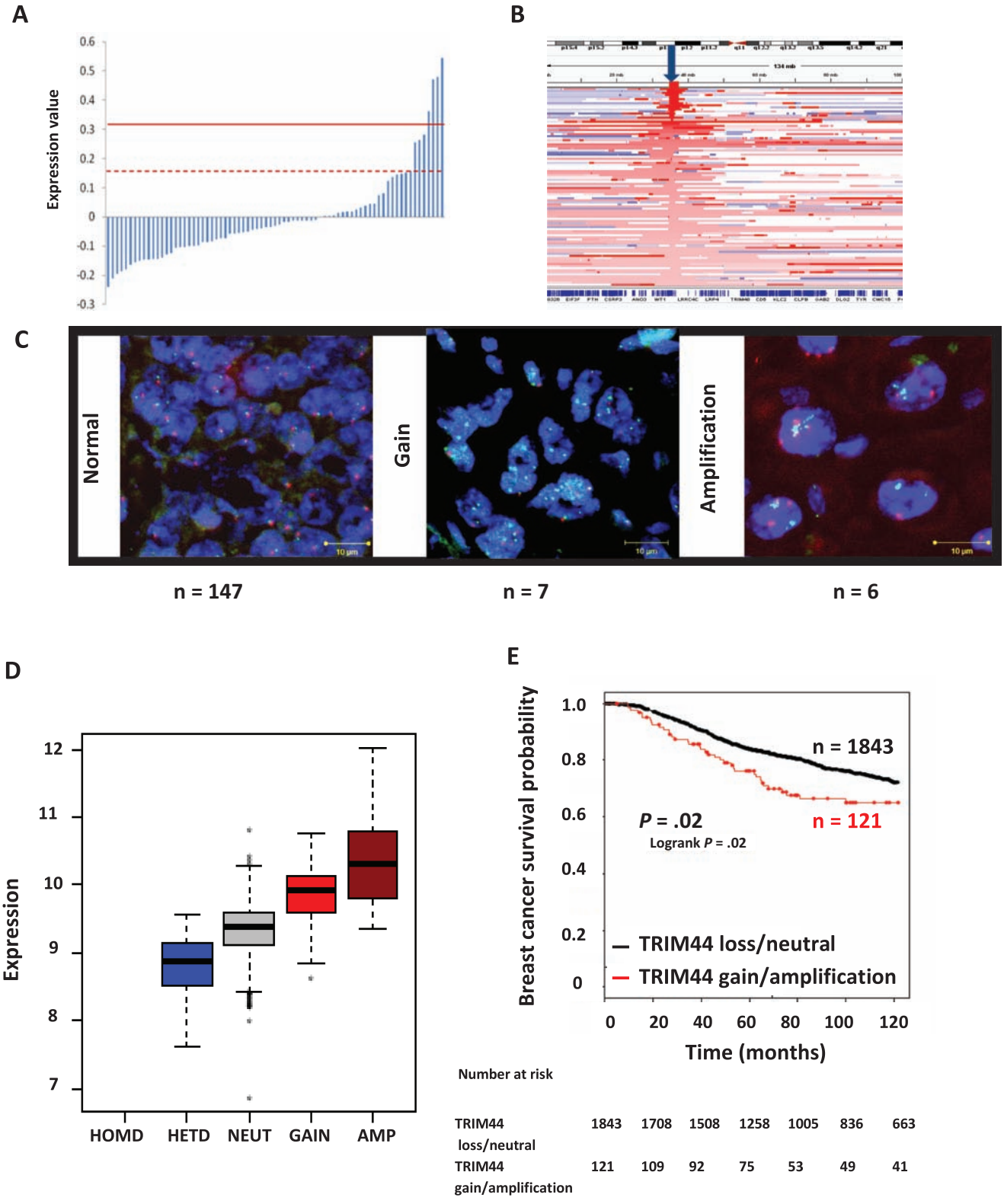

Figure 2. Correlation of TRIM44 expression, copy number, and survival. **A**) Expression of TRIM44 in 75 esophago-gastric cancers (EGCs) plotted on a log10 scale. **Dotted red line** and **solid red line** segregate tumors with more than 1 standard deviation and more than 2 standard deviations of TRIM44 expression relative to the rest of the tumors. **B**) Heat map showing the copy number status of 1932 tumors on Tumorscape (various different tumor types). **Blue arrow** shows the location of *TRIM44* on chromosome 11. **C**) Representative fluorescent in situ hybridization images performed on tissue microarrays of EGCs. The individual **green** and **red signals** indicate *TRIM44* and chromosome 11 centromeric probes, respectively. **D**) Box and whisker plots correlating expression and copy number status of TRIM44 in the METABRIC cohort (21) consisting of 1980 breast tumors. *P* value computed by one-sided Jonckheere–Terpstra test. AMP = amplifications; GAIN = gain in copy numbers; HETD = heterozygously deleted; HOMD = homozygously deleted; NEUT = neutral. **E**) Kaplan–Meier curve comparing survival of patients with gains and amplifications of *TRIM44* to patients with loss or normal copy number of *TRIM44* (n = 1980; *P* value computed by two-sided log rank test). The survival information was not available for 16 patients.

Table 1. Breakdown of frequency of *TRIM44* amplifications of different tumor subtypes in Tumorscape

Cancer subset	No.	Frequency of amplification, %	
		Overall	Focal
All cancers	3131	12.0	3.0
All epithelial cancers	1932	16.1	4.0
Breast	243	19.8	6.2
Lung, all subtypes	774	16.0	4.8
Lung, non–small cell	733	16.1	4.8
Lung, small cell	40	15.0	5.0
Colorectal	161	16.8	0.6
Esophageal, squamous	44	15.9	4.6
Ovarian	103	12.6	4.9
Glioma	41	7.3	0.0
All neural	217	6.5	0.9
Hepatocellular	121	5.8	0.8
Medulloblastoma	128	3.9	0.8
Melanoma	111	18.0	0.9
Renal	699	9.5	0.8
Prostate	92	8.7	2.2
All hematological	126	2.3	0.1
Acute lymphoblastic leukemia	391	3.3	0.3
Myeloproliferative disorder	215	0.0	0.0

the proportion of patients with TRIM44 overexpression (P = .04) (Supplementary Figure 1, available online). However, FISH performed on a tissue microarray of Barrett's tissue failed to identify any *TRIM44* amplifications (n = 78; data not shown). Taken together, although TRIM44 overexpression can occur early in EGC pathogenesis, *TRIM44* amplification is a late genomic event causing overexpression.

Because Tumorscape suggested that *TRIM44* amplification was most common in BC (19.8% overall; 6.2% focal) (Table 1), we further validated these findings by analyzing copy number and transcriptomic data in an independent set of 1980 BCs (METABRIC) (21). Of patients in this cohort, 6.1% had *TRIM44* amplifications and gains, and expression was also copy number driven (P < .001 by Jonckheere–Terpstra test) (Fig 2D). Consistently, BC patients with *TRIM44* gains and amplifications had a statistically significantly poorer prognosis than patients with normal copy number (hazard ratio [HR] = 1.49; 95% confidence interval [CI] = 1.06 to 2.08; P = .02) (Figure 2E).

Driver Status of *TRIM44* in 11p13 Amplicon

To assess whether *TRIM44* is a driver of the 11p13 amplicon, we looked at the minimal common region analysis in the original article describing the METABRIC dataset (21). This showed that *TRIM44* lies in the minimal common regions of alteration in both estrogen receptor–positive and –negative breast cancers as well as in the basal-like subgroup (Supplementary Table 5, available online). In addition, we used an in vitro approach to elucidate the driver gene status of *TRIM44*. First, we identified a cell line (HSC39) with high-level amplifications of *TRIM44*. Single nucleotide polymorphism 6 profiling of HSC39 showed that there was high-level amplification encompassing 1.2 Mb in chromosomal region 11p13 (Figure 3A). This amplicon encompassed only eight genes: *APIP*, *PDHX*, *CD44*, *SLC1A2*, *PAMR1*, *FJX1*, *TRIM44*, and *LDLRAD3*. FISH performed on metaphase preparations of HSC39 showed double minute amplifications of *TRIM44* (Figure 3B).

We then performed an siRNA screen knocking down all genes within the 11p13 amplicon in HSC39. This showed that knockdown of CD44, FJX1, and TRIM44 led to a decrease of more than 50% cellular proliferation compared with control siRNA (Figure 3C). The median fractions of cells surviving knockdown of TRIM44, CD44, and FJX1 were 0.172, 0.190, and 0.337, respectively. Taken together, the prognostic significance of *TRIM44* amplification, the minimal common region analysis using METABRIC, and the siRNA screen suggest that *TRIM44* is indeed a driver gene in the amplicon.

Identification of Enriched Pathways Associated With TRIM44 Overexpression

To identify potential therapeutic options for patients with TRIM44 amplifications, we performed GSEA (18) to identify associations between pathway activity and TRIM44, ranking genes by correlation with TRIM44 expression in two publicly available EGC gene expression datasets (Kim: n = 64, Greenawalt: n = 37) (25,26). Of all pathways tested for association, mTOR was the only statistically significant overenriched pathway in the Greenawalt dataset (P = .02) and was one of the three statistically significant overenriched pathways in the Kim dataset (mTOR: P = .04; Hypoxia: P = .02; Wnt: P = .04) (Figure 4A). Combining both datasets, the mTOR pathway was the most statistically significant overenriched pathway (Supplementary Table 6, available online). To validate these findings, we repeated GSEA on the METABRIC cohort. In BC, two pathways (mTOR: P < .001; Wnt: P = .03) were overenriched (Figure 4B). However, only enrichment of the mTOR pathway reached statistical significance with multiple testing (false discovery rate Q value = 0.05) (Supplementary Table 7, available online).

To further confirm a link between TRIM44 and mTOR activity, we performed gene expression profiling of HSC39 after siRNA knock-down. TRIM44 knockdown caused a decreased enrichment in the mTOR signature compared with cells treated with control siRNA (normalised enrichment score (NES) = –1.46; P < .001) (Figure 4C; Supplementary Table 8, available online). In addition, siRNA knockdown of TRIM44 in HSC39 and another TRIM44-amplified line (SNU16) (Supplementary Figure 2, available online) caused a decrease in AKT phosphorylation at S473 and P70S6K phosphorylation at T389 (Figure 4D), consistent with our GSEA findings that TRIM44 overexpression leads to high mTOR activity. To complement the genetic analysis and demonstrate the association between TRIM44 and mTOR in the clinical setting, we performed GSEA on METABRIC samples with high expression (top 25%) combined with samples with gains and amplifications vs samples with normal copy number. The mTOR pathway was the only statistically overenriched pathway in TRIM44-overexpressing samples (Supplementary Table 9, available online).

Validation of High mTOR Activity in *TRIM44*-Amplified EGC Samples

Next, we asked whether amplification of TRIM44 increased mTOR activity in primary EGC patient samples using immunohistochemistry. We stained all samples in which we had successfully

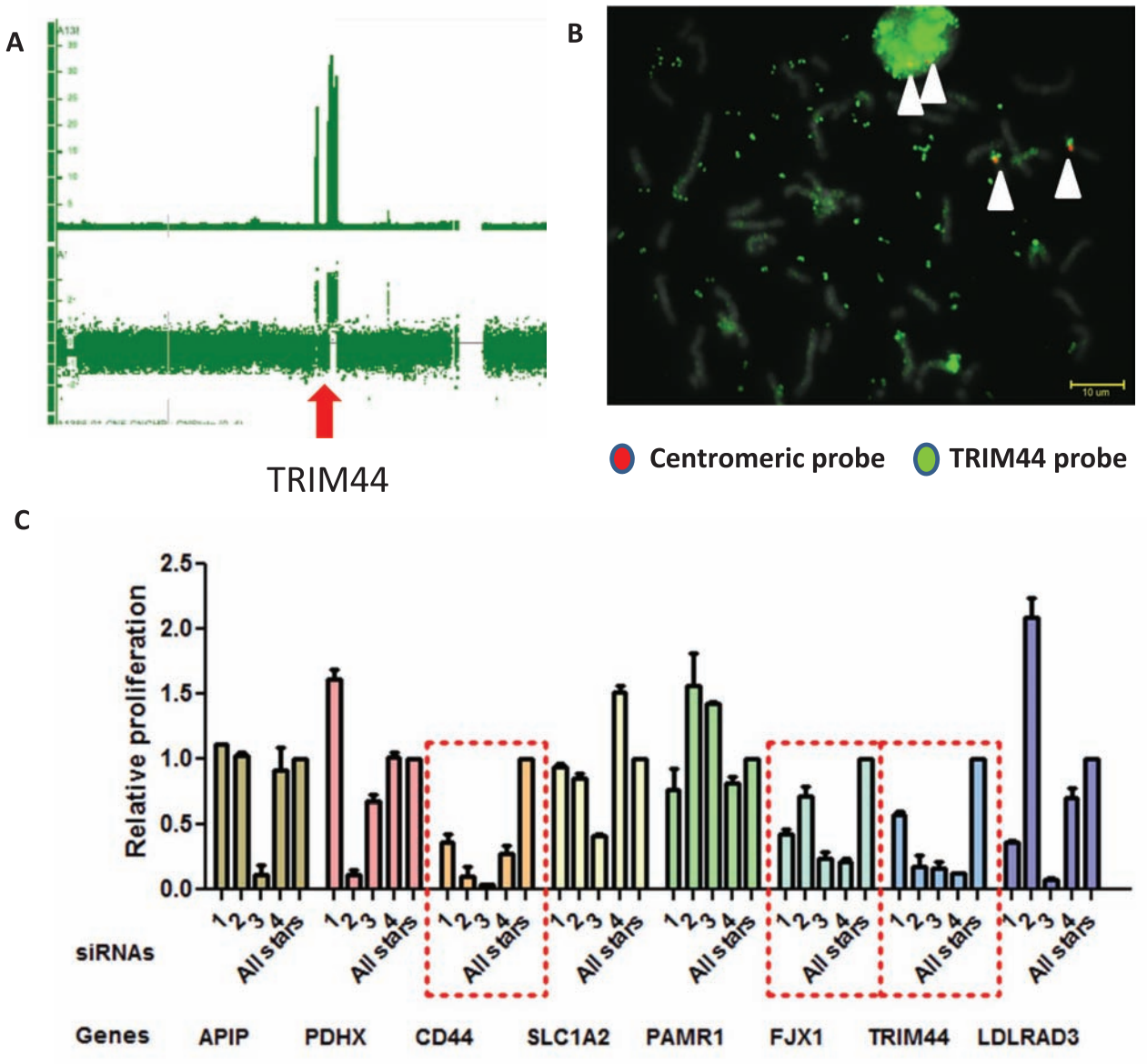

Figure 3. Minimal common region of amplification and effect of gene-specific knockdown across the amplicon. **A**) Minimal common region analysis of the 11p13 amplicon. **Arrow** indicates the position of TRIM44. **B**) Representative images of fluorescent in situ hybridization performed on metaphase preparations of HSC-39. The individual **green** and **red signals** indicate *TRIM44* and chromosome 11 centromeric probes, respectively. The **white arrows** point to the centromeric probe. **C**) siRNA screen performed for eight genes present in the double minute amplifications in HSC39. **Red squares** highlight the three genes (*CD44, FJX1*, and *TRIM44*) that showed more than 50% decrease in proliferation of cells relative to treatment with control siRNA with at least three siRNAs. The screen was performed with three technical triplicates and three biological repeats for each siRNA transfection.

performed a FISH assay for *TRIM44* (n = 160). All patients with gross *TRIM44* amplifications (n = 6) had diffuse staining of p-mTOR staining, which corresponded to TRIM44 staining (Supplementary Figure 3, available online). The proportion of patients with increased *TRIM44* copy number with p-mTOR positivity (n = 9 of 13) was statistically significantly higher than the proportion of patients with normal copy number of *TRIM44* and p-mTOR positivity (n = 52 of 147; P = .03) (Figure 5A). Furthermore, immunofluorescent costaining with TRIM44 and p-mTOR in one exemplar patient showed that TRIM44 and p-mTOR staining colocalized within the same cells (Figure 5B). Interestingly, in one patient sample with *TRIM44* amplification, TRIM44 staining intensity was highly heterogenous. Areas staining strongly for TRIM44 also displayed high levels of mTOR activity, as tested by staining for p-mTOR, p-P70S6K, and p-4EBP1 protein levels (Figure 5C), whereas TRIM44 low-expressing cells in this tumor had low levels of mTOR activity. Taken together, these data provide further evidence that TRIM44-overexpressing cells have high mTOR activity.

Effectiveness of mTOR Inhibitors in Treating *TRIM44*-Amplified Tumors

siRNA knockdown of TRIM44 in *TRIM44*-amplified cells causes a decrease in proliferation. However, treatment with siRNAs still

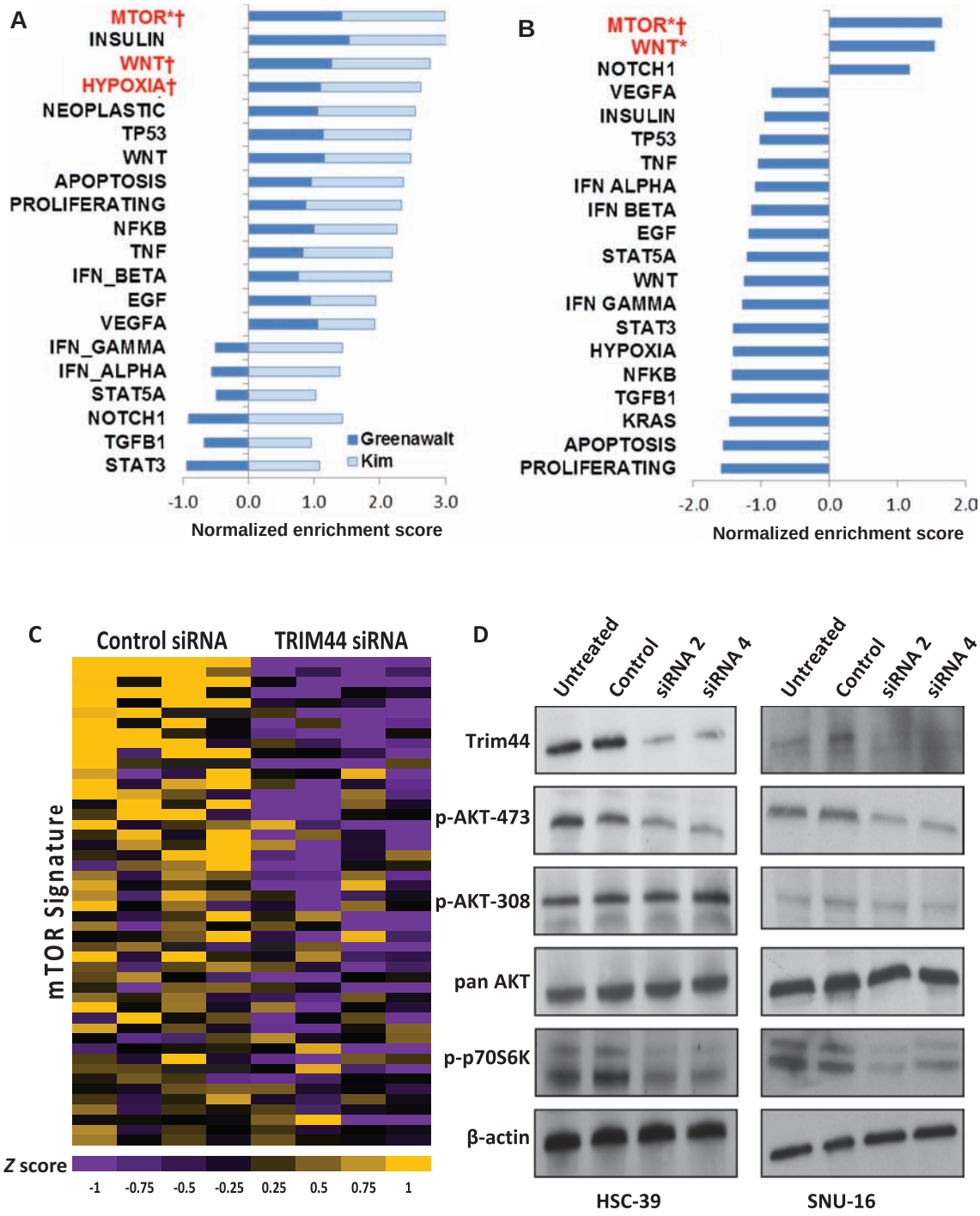

Figure 4. Association of TRIM44 overexpression and mTOR activity. **A**) Identification of pathway signatures enriched in esophago-gastric cancer (EGC) patients with TRIM44 overexpression (ranking genes by correlation with TRIM44 expression in two publicly available independent EGC gene expression datasets). Pathways are ranked by the *P* value of enrichment. *Statistically enriched pathways enriched in the Greenawalt dataset (26). †Statistically enriched pathways in the Kim dataset (25). Normalized enrichment score indicates strength of enrichment. Scores greater than 0 indicate overenrichment and pathway activation, and scores less than 0 indicate underenrichment and pathway suppression. **B**) Validation of enriched pathway signatures in the METABRIC cohort (ranking genes by correlation with TRIM44 expression in the METABRIC cohort). Pathways are ranked by the *P* value of enrichment. *Statistically significantly enriched by nominal *P* value. †Statistically significantly enriched by false discovery rate–corrected *Q* value. Normalized enrichment score indicates strength of enrichment. Scores greater than 0 indicate overenrichment and pathway activation, and scores less than 0 indicate underenrichment and pathway suppression. *P* values obtained using gene set enrichment analysis (GSEA), which is based on an ad hoc modification of the two-sided KS test. **C**) Heatmap for expression of genes in the mTOR signature upon small interfering RNA (siRNA) knockdown in the *TRIM44*-amplified cell line HSC39. The samples included HSC39 cells treated with two independent TRIM44 siRNAs (in duplicate) and HSC39 treated with All Stars Negative siRNA (in quadruplicate), making a total of eight samples. The **bars** represent the scaled *Z* score values (using median and median of absolute deviation) of gene expression of the 48 most highly enriched genes involved in the mTOR signature (genes in the leading edge analysis of the GSEA and with a *P* value less than .01 in the original paper generating the signature, Molecular signatures database (MSigDB) Broad Institute, http://www.broadinstitute.org/gsea/msigdb/index.jsp, [also Ref. 18]). **Gold** represents high expression; **purple** represents low expression. **D**) Immunoblot of *TRIM44*-amplified cell lines (HSC-39 and SNU16) after siRNA knockdown for TRIM44 and components of the AKT and mTOR signaling pathway.

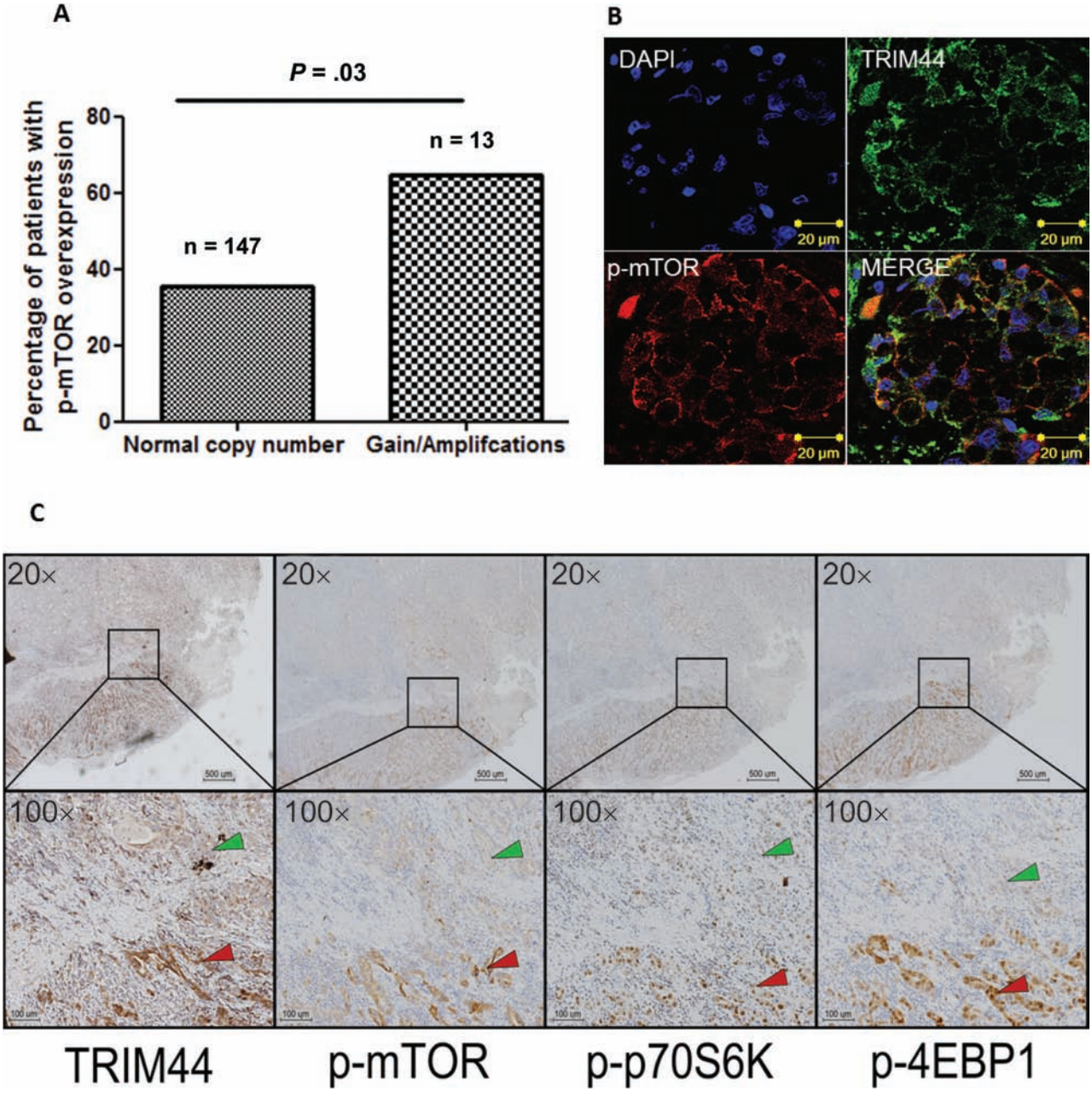

Figure 5. Comparison of TRIM44 and p-mTOR staining in patient samples. **A**) Percentage of patients with p-mTOR positivity stratified by TRIM44 amplification and gain status. *P* value computed by two-sided Fisher exact test. **B**) Immunofluorescence staining of TRIM44 and p-mTOR in patient 3875. **C**) Immunohistochemistry performed on patient 8312 for TRIM44 p-mTOR, p-P70S6K, and p-4EBP1 staining in the primary tumor. **Red arrows** show cells with high expression of TRIM44 and high mTOR activity, whereas the **green arrows** show the cells with low TRIM44 expression and low mTOR activity. All statistical tests were two-sided.

requires further development before it can be used in clinical practice (27). Hence we sought to explore whether any small molecules and drugs could recapitulate the effects of siRNA knockdown in *TRIM44* amplified cells. To do this, we used our siRNA perturbation experiment to perform an analysis using the connectivity map (20). Using this approach, we discovered that the TRIM44 overexpression gene signature consistently could be most effectively reversed by inhibitors targeting the PI3kinase–AKT–mTOR pathway (Table 2).

To test this prediction, we treated the amplified lines SNU-16 and HSC-39 with wortmannin (PI3K inhibitor), everolimus (clinically licensed mTOC1 inhibitor), and PP242 (mTORC1 and mTORC2 inhibitor). Everolimus treatment resulted in 88% and 70% inhibition of cell proliferation in SNU-16 and HSC-39, respectively. Conversely, treatment of OE19, which has low levels of TRIM44, with everolimus resulted in only 35% inhibition of cellular proliferation even at high doses (Figure 6A). These inhibition results could also be recapitulated in vivo. Everolimus treatment of HSC-39 xenografts resulted in a decrease in xenograft size (n = 3 in each arm; *P* = .05) (Figure 6, B and C), as well as a corresponding decrease in the levels of phosphorylated P70S6K (Figure 6D). Treatment of OE19 xenografts with everolimus had no demonstrable effect (n = 5 in each arm) (Figure 6E).

Table 2. Drugs capable of altering the TRIM44 signature-derived HSC-39 cells treated with TRIM44 small interfering RNA

Drug	No. of experiments	Drug type	Rank	Enrichment	*P*
MG-262	3	Proteasome inhibitor	1	−0.99	<.001
GW-8510	4	CDK2 inhibitor	2	0.98	<.001
trichostatin A	182	HDAC inhibitor	3	0.64	<.001
Wortmannin	18	PI3K inhibitor	4	0.57	<.001
LY-294002	61	PI3K inhibitor	5	0.52	<.001
Sirolimus	44	mTOR inhibitor	6	0.47	<.001
Vorinostat	12	HDAC inhibitor	7	0.65	<.001
Pizotifen	4	Seratonin antagonist	8	−0.90	<.001
Doxylamine	5	Antihistamine	9	−0.81	<.001
Quinostatin	2	PI3K inhibitor	10	0.98	<.001
Colforsin	5	PKA activator	11	0.78	.001
Leflunomide	4	Pyrimidine synthesis inhibitor	12	0.83	.001
5707885	4	Unlisted	13	0.83	.001
5224221	2	Unlisted	14	0.97	.002
STOCK1N-35696	2	Unlisted	15	−0.97	.002
Benperidol	4	Antipsychotic	16	−0.82	.002
CP-645525-01	3	Unlisted	17	0.89	.002
BCB000040	4	Unlisted	18	0.81	.003
MS-275	2	HDAC inhibitor	19	0.96	.003
STOCK1N-28457	3	Unlisted	20	−0.88	.003

Effect of PI3K Inhibitors in *TRIM44*-Amplified Cell Lines

Treatment with PP242 (dual mTORC1 and mTORC2 inhibitors) showed that HSC39 and SNU16 cells remained more susceptible to PP242 but very high doses of PP242 leds to cell death in OE19. Using 100 nm of each inhibitor, we further demonstrated that HSC39 and SNU16 were more susceptible to everolimus and PP242 treatment than OE19. However, this was not the case for wortmannin (Supplementary Figure 4, available online). Taken together, these data suggest that targeting the mTOR pathway is more effective in *TRIM44*-amplified cell lines compared with inhibition of the PI3K pathway.

Discussion

EGC is a highly lethal disease with a rapidly rising incidence in the Western world (28,29). Current clinical staging algorithms cannot prognosticate patients accurately. Hence, we previously attempted to identify molecular prognostic markers to aid clinical staging (12,16). To this end, we have identified TRIM44 as a highly prognostic biomarker in EGC. Patients with overexpression of TRIM44 had a statistically significantly poorer prognosis compared with patients with wild-type levels of TRIM44. In this study, we identified genomic amplification as a basis for TRIM44 overexpression in EGC. In addition, interrogation of the METABRIC dataset showed that *TRIM44* amplification is common in BC and similarly confers a poor prognosis.

Although accurate prognostication can help with informed clinical decision making in oncology, it does not provide any tangible benefits to patients. At one end of the spectrum, patients staged as having an early stage and "biologically favorable" tumor can be simply reassured; on the other hand, there is no additional therapy available for patients predicted to have a poor prognosis from molecular stratification. The exact function of TRIM44 is unknown, rendering it more difficult to exploit for therapy. However, our previous work showed that TRIM44 overexpression confers a poor prognosis, and we have now taken this observation further and showed that it is commonly amplified in epithelial cancers. From a therapeutic perspective, we hypothesized that *TRIM44* amplification and overexpression can lead to pathway activation within tumors. In silico analysis using GSEA provided us with a link between TRIM44 overexpression and high mTOR activity. This was validated using in vitro and in vivo experiments. More important, our study provides preclinical evidence that mTOR inhibition could potentially be used to treat *TRIM44*-amplified tumors. Although our analysis was limited to EGCs and BCs, it would be tempting to speculate that mTOR inhibitors could be used to treat other cancer subtypes harboring *TRIM44* amplifications.

The strength of this work lies in our ability to interrogate large clinical resources of genomic and expression microarray data to dissect the genetic basis of TRIM44 overexpression. We also had a large resource of preneoplastic samples, cancer, and metastatic tumors with clear clinical follow-up, which allowed us to interrogate the molecular expression of TRIM44 in various stages of the disease process. In addition, this study highlights the importance of the continuation of work on newly discovered prognostic markers to discover novel therapeutic strategies.

There are limitations to our study. Similar to the case of Her2, genomic amplification is not the only explanation for protein overexpression. Potential mechanisms leading to TRIM44 overexpression could be through transcriptional regulation by c-myc or FOXA1. c-myc and FOXA1 are two transcriptional factors dysregulated in EGCs and both have binding sites within the promoter region of *TRIM44* (30,31). Data from the EGC International Cancer Genome Consortium showed no mutations of *TRIM44* in 66 tumors, and hence activation of *TRIM44* by point mutations is unlikely (unpublished observations, http://dcc.icgc.org). Although we have focused on the therapeutic potential of mTOR inhibitors in *TRIM44*-amplified cell lines, it is possible that patients who have normal copy TRIM44-overexpressing tumors could benefit from mTOR inhibition. This area merits

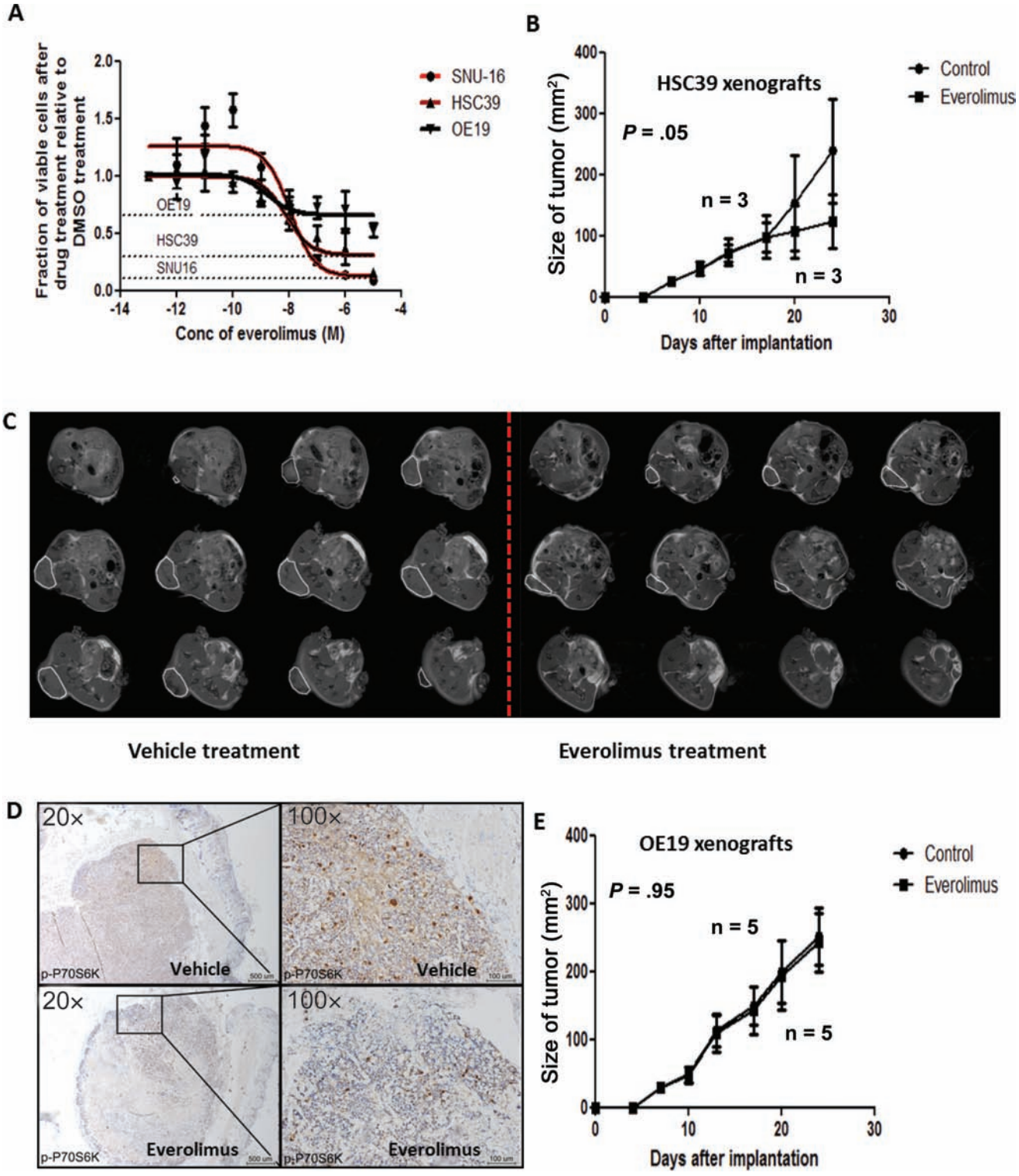

Figure 6. Treatment of *TRIM44*-amplified cells with mTOR inhibitors in vitro and in vivo. **A**) Effect of everolimus (mTOR inhibitor) on two amplified cell lines (HSC39 and SNU-16) and a low TRIM44-expressing cell line (OE19). The **dotted lines** represent the maximum inhibition of the cells relative to dimethyl sulfoxide-treated cells. All experiments were repeated at least three times. **B**) Comparison of HSC39 xenograft size in mice treated with everolimus or control (assessed using calliper measurements). Error bars represent ± standard deviation; n = 3. **C**) Magnetic resonance imaging of HSC39 xenografts in nude mice. **Left panel** shows the size of xenografts treated with vehicle control, and **right panel** shows the size of xenografts treated with everolimus. The **circles** in the figures mark out the xenografts on magnetic resonance imaging. **D**) HSC39 xenografts from everolimus-treated mice and control mice were harvested and stained for p-P70S6K. **E**) Effect of everolimus treatment on OE19 xenografts in mice. *P* value computed by two-sided Student *t* test. Error bars represent ± standard deviation; n = 5 in each group.

further investigation. Further work is also required to understand the mechanism underlying TRIM44 overexpression and high mTOR activity. In addition, our in silico analysis shows that TRIM44 overexpression is also correlated with high WNT activity. It is plausible that TRIM44 overexpression activates both the WNT and mTOR pathways simultaneously and that this has synergistic effects on tumor aggressiveness. It is noteworthy that our cell line model HSC-39, which has double minute amplifications of *TRIM44*, has a truncated β-catenin. Kawanishi et al. previously reported a deletion in the mRNA sequence of β-catenin in HSC-39, which is responsible for loss of normal cadherin function (32). Although this finding is cell-line specific, it suggests that TRIM44 can potentially activate the mTOR signalling cascade independently of the WNT pathway. This work is complex and ongoing and is beyond the scope of this clinically focused article (33).

In conclusion, these data highlight the utility of genomic data curated across multiple cancer sites to inform therapy decisions in oncology. We have demonstrated that *TRIM44* is commonly amplified in EGCs and BCs. Using a combination of genomic, functional, gene expression, and in vivo approaches, we have shown that TRIM44-overexpressing tumors have hyperactive mTOR signalling and mTOR inhibition may provide a therapeutic strategy for *TRIM44*-amplified tumors.

References

1. Ludwig JA, Weinstein JN. Biomarkers in cancer staging, prognosis and treatment selection. *Nat Rev Cancer*. 2005;5(11):845–856.
2. McShane LM, Altman DG, Sauerbrei W, et al. REporting recommendations for tumour MARKer prognostic studies (REMARK). *Br J Cancer*. 2005;93(4):387–391.
3. Altman DG, McShane LM, Sauerbrei W, et al. Reporting Recommendations for Tumor Marker Prognostic Studies (REMARK): explanation and elaboration. *PLoS Med*. 2012;9(5):e1001216.
4. Hemingway H, Croft P, Perel P, et al. Prognosis research strategy (PROGRESS) 1: a framework for researching clinical outcomes. *BMJ*. 2013;346:e5595.
5. Riley RD, Hayden JA, Steyerberg EW, et al. Prognosis Research Strategy (PROGRESS) 2: prognostic factor research. *PLoS Med*. 2013;10(2):e1001380.
6. Slamon D, Eiermann W, Robert N, et al. Adjuvant trastuzumab in HER2-positive breast cancer. *N Engl J Med*. 2011;365(14):1273–1283.
7. Mitsudomi T, Morita S, Yatabe Y, et al. Gefitinib versus cisplatin plus docetaxel in patients with non-small-cell lung cancer harbouring mutations of the epidermal growth factor receptor (WJTOG3405): an open label, randomised phase 3 trial. *Lancet Oncol*. 2010;11(2):121–128.
8. Chapman PB, Hauschild A, Robert C, et al. Improved survival with vemurafenib in melanoma with BRAF V600E mutation. *N Engl J Med*. 2011;364(26):2507–2516.
9. Druker BJ, Talpaz M, Resta DJ, et al. Efficacy and safety of a specific inhibitor of the BCR-ABL tyrosine kinase in chronic myeloid leukemia. *N Engl J Med*. 2001;344(14):1031–1037.
10. Bang YJ, Van Cutsem E, Feyereislova A, et al. Trastuzumab in combination with chemotherapy versus chemotherapy alone for treatment of HER2-positive advanced gastric or gastro-oesophageal junction cancer (ToGA): a phase 3, open-label, randomised controlled trial. *Lancet*. 2010;376(9742):687–697.
11. Maemondo M, Inoue A, Kobayashi K, et al. Gefitinib or chemotherapy for non-small-cell lung cancer with mutated EGFR. *N Engl J Med*. 2010;362(25):2380–2388.
12. Ong C-AJ, Shapiro J, Nason KS, et al. Three-gene immunohistochemical panel adds to clinical staging algorithms to predict prognosis for patients with esophageal adenocarcinoma. *J Clin Oncol*. 2013;31(12):1576–1582.
13. Kashimoto K, Komatsu S, Ichikawa D, et al. Overexpression of TRIM44 contributes to malignant outcome in gastric carcinoma. *Cancer Sci*. 2012;103(11):2021–2026.
14. Ozato K, Shin D-M, Chang T-H, et al. TRIM family proteins and their emerging roles in innate immunity. *Nat Rev Immunol*. 2008;8(11):849–860.
15. Hatakeyama S. TRIM proteins and cancer. *Nat Rev Cancer*. 2011;11(11):792–804.
16. Peters CJ, Rees JR, Hardwick RH, et al. A 4-gene signature predicts survival of patients with resected adenocarcinoma of the esophagus, junction, and gastric cardia. *Gastroenterology*. 2010;139(6):1995–2004 e15.
17. Paterson AL, Shannon NB, Lao-Sirieix P, et al. A systematic approach to therapeutic target selection in oesophago-gastric cancer. *Gut*. 2013;62(10):1415–1424.
18. Subramanian A, Tamayo P, Mootha VK, et al. Gene set enrichment analysis: a knowledge-based approach for interpreting genome-wide expression profiles. *Proc Natl Acad Sci U S A*. 2005;102(43):15545–15550.
19. Parent R, Kolippakkam D, Booth G, et al. Mammalian target of rapamycin activation impairs hepatocytic differentiation and targets genes moderating lipid homeostasis and hepatocellular growth. *Cancer Res*. 2007;67(9):4337–4345.
20. Lamb J, Crawford ED, Peck D, et al. The Connectivity Map: using gene-expression signatures to connect small molecules, genes, and disease. *Science (New York, N Y)*. 2006;313(5795):1929–1935.
21. Curtis C, Shah SP, Chin S-F, et al. The genomic and transcriptomic architecture of 2,000 breast tumours reveals novel subgroups. *Nature*. 2012;486(7403):346–352.
22. Reid BJ, Li X, Galipeau PC, et al. Barrett's oesophagus and oesophageal adenocarcinoma: time for a new synthesis. *Nat Rev Cancer*. 2010;10(2):87–101.
23. Vogelstein B, Kinzler KW. Cancer genes and the pathways they control. *Nat Med*. 2004;10(8):789–799.
24. Beroukhim R, Mermel CH, Porter D, et al. The landscape of somatic copy-number alteration across human cancers. *Nature*. 2010;463(7283):899–905.
25. Kim SM, Park YY, Park ES, et al. Prognostic biomarkers for esophageal adenocarcinoma identified by analysis of tumor transcriptome. *PLoS One*. 2010;5(11):e15074.
26. Greenawalt DM, Duong C, Smyth GK, et al. Gene expression profiling of esophageal cancer: comparative analysis of Barrett's esophagus, adenocarcinoma, and squamous cell carcinoma. *Int J Cancer*. 2007;120(9):1914–1921.
27. Pecot CV, Calin GA, Coleman RL, et al. RNA interference in the clinic: challenges and future directions. *Nat Rev Cancer*. 2011;11(1):59–67.
28. Pohl H, Sirovich B, Welch HG. Esophageal adenocarcinoma incidence: are we reaching the peak? *Cancer Epidemiol Biomarkers Prev*. 2010;19(6):1468–1470.
29. Siegel R, Naishadham D, Jemal A. Cancer statistics, 2012. *CA Cancer J Clin*. 2012;62(1):10–29.
30. Sarbia M, Arjumand J, Wolter M, et al. Frequent c-myc amplification in high-grade dysplasia and adenocarcinoma in Barrett esophagus. *Am J Clin Pathol*. 2001;115(6):835–840.
31. Lin L, Miller CT, Contreras JI, et al. The hepatocyte nuclear factor 3 alpha gene, HNF3alpha (FOXA1), on chromosome band 14q13 is amplified and overexpressed in esophageal and lung adenocarcinomas. *Cancer Res*. 2002;62(18):5273–5279.
32. Kawanishi J, Kato J, Sasaki K, et al. Loss of E-cadherin-dependent cell-cell adhesion due to mutation of the beta-catenin gene in a human cancer cell line, HSC-39. *Mol Cell Biol*. 1995;15(3):1175–1181.
33. Ong C A J SNB, Skehel J M, et al. Utilizing integrative genomic analysis and proteomics to decipher the biology and therapeutic potential of TRIM44 in oesophageal adenocarcinoma and breast cancer. *Gut*. 2013;62 (Supplement 1).

Funding

This work was supported by the Singapore National Research Foundation under its NRF-MOH overseas scholarship and administered by the Singapore Ministry of Health's National Medical Research Council to C.A.J. Ong. This research was supported by the Medical Research Council, Cambridge Experimental Cancer Medicine Centre, and the NIHR Cambridge Biomedical Research Centre.

Notes

C-A. J. Ong and N.B. Shannon contributed equally to this work.

The content is solely the responsibility of the authors and does not necessarily represent the official views of the Medical Research Council, the National Institute of Health, or the Singapore Ministry of Health's National Medical Research Council. The funders had no role in study design, data collection and analysis, decision to publish, or preparation of the manuscript.

We would like to thank Dr P. Lao-Sirieix, Dr J. Shields, Mr C. Peters, Dr X.Y Goh, Dr R. O'Neill, and Dr M. de la Roche for their advice and technical help. We would also like to thank Dr Anna Paterson and Dr Sibu Varghese for obtaining preneoplastic samples and Dr Yanagihara for the generous gift of HSC-39. Special thanks also go to the Department of Gastroenterology (UCL, London), Department of Pathology (UCL, London), and all members of the OCCAMS collaboration for collection of clinical samples and information. In addition, we would like to thank members of the Esophageal International Cancer Genome Consortium (funded by Cancer Research UK) for generating sequencing data of EGC.

Affiliations of authors: MRC Cancer Unit, Cambridge, UK (C-AJO, CSR-I, MO, CEW, AN, RCF); Cancer Research UK Cambridge Institute, Cambridge, UK (NBS, OMR, D-eH, MIK, CC, KB); UK Cambridge Esophagogastric Centre, Addenbrooke's Hospital, Cambridge, UK (RHH).